ELSEVIER

Carbohydrate Polymers 36 (1998) 67–72

Carbohydrate Polymers

# Characterising semi-refined *iota*-carrageenan networks by atomic force microscopy

A.P. Gunning[a], P. Cairns[a], A.R. Kirby[a], A.N. Round[a], H.J. Bixler[b], V.J. Morris[a,*]

[a]*Institute of Food Research, Food Biophysics Department, Norwich Research Park, Colney, Norwich NR4 7UA, UK*
[b]*Shemberg Corporation, Packnaan, Mandaue City, Cebu City, The Phillipines 6014.*

Received 11 April 1997; revised 22 July 1997; accepted 22 July 1997

**Abstract**

Samples of PNG *iota* carrageenan have been studied by X-ray diffraction and Atomic Force Microscopy (AFM). Aqueous preparations of PNG *iota* carrageenan can be fractionated into water soluble and water insoluble components. The water soluble component is largely composed of *iota* carrageenan containing small amounts of cellulose. AFM studies reveal that this component forms network structures very similar to those obtained for refined *iota* carrageenan. Some swollen cellulosic networks were observed in the PNG samples. The water insoluble fraction has been shown to be predominately partially crystalline cellulose I. AFM reveals that the cellulose is present as a fibrous network similar to that found for bacterial cellulose or the cellulosic component of plant cell walls. In the PNG samples the lateral ordering of the cellulose microfibrils has been disrupted presumably during the extraction of the PNG carrageenan from the seaweed. The AFM imaging conditions used to study the insoluble component would not permit imaging of any *iota* carrageenan networks which may be present in this sample. 

*Keywords:* Atomic Force Microscopy; AFM; PNG carrageenan; Semi-refined carrageenan; Plant cell walls; Bacterial cellulose; X-ray diffraction

## 1. Introduction

Carrageenans are a family of sulphated polysaccharides extracted from red marine algae (*Rhodophyceae*) and used industrially as gelling and thickening agents (Percival & McDowell, 1967; Rees, 1969). The extracted polysaccharides can be classified into four major types (*iota, kappa, lambda* and furcellaran) depending on their level and type of sulphate substitution (Percival & McDowell, 1967; Rees, 1969). The idealised repeat unit for iota carrageenan is shown in Fig. 1. The major source of *iota* carrageenan is from the seaweed *Eucheuma spinosum*, which is farmed commercially in the Philippines. The traditional extraction approach involves boiling the seaweed in alkali in order to dissolve out the carrageenan and increase its gel strength (Phillips, 1996; Tye, 1994). In the preparation of PNG (Philippino Natural Grade, sometimes called semi-refined or alternatively refined) carrageenan, the alkali treatment step is milder, involving steeping washed sundried seaweed in alkali at moderate temperature (Phillips, 1996; Tye, 1994). The latter process does not dissolve out the carrageenan and the resultant product after washing and drying stages will contain cellulose from the plant cell wall.

Hoffman et al. (1995) have examined the effect of extraction procedures on the composition and properties of *kappa* carrageenan isolated from *E. cottoni* seaweed. Using mild extraction procedures, similar to those in the preparation of PNG *kappa* carrageenan, they demonstrated the presence of cellulose in the final product. From X-ray diffraction and solid-state NMR studies it was concluded that the cellulose was partially crystalline and in the cellulose I form (Hoffman et al., 1995). It was suggested that the cellulose was probably present in a microfibrillar form.

In the present studies reported here we have examined samples of PNG *iota* carrageenan. X-ray diffraction has been used to confirm the presence of cellulose in the cellulose I form. Atomic Force Microscopy (AFM) has been used to visualise the carrageenan and cellulosic networks formed by this material and to demonstrate the fibrous nature of the cellulose component. The carrageenan network has been compared with the network structures formed from traditionally refined iota carrageenan. The cellulosic networks have been compared with those found in higher plant cell walls and those secreted by *Acetobacter xylinum*.

* Author to whom correspondence should be addressed.

0144-8617/98/$19.00 
*PII* S0144-8617(97)00112-4

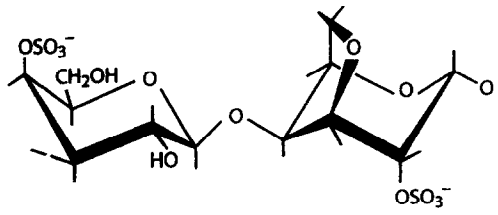


Fig. 1. Idealised disaccharide repeat unit for *iota* carrageenan.

## 2. Materials and methods

The sample of PNG *iota* carrageenan was S-100 (lot number 951118/5). The PNG carrageenan had been obtained by extracting sundried seaweed using 8% KOH at 70°C. This step removes most of the colour, protein and lipid leaving behind the carrageenan–cellulose matrix and some organic salts. This extract was washed several times in cold water, dried and ground to a fine powder to make the commercial product from which the present sample was obtained. This sample was dispersed in water at a concentration of 1 $mgml^{-1}$: the sample was dispersed in deionised water and stirred, heated to 95–100°C for 10 min., and then cooled to room temperature. The resulting dispersion was turbid. On standing it separated into a clearer supernatant and an 'insoluble deposit'. The supernatant and the deposit were separated and each divided into two fractions. One fraction was freeze-dried and later used for X-ray diffraction studies. The other fraction was used to prepare specimens for AFM studies. The aqueous dispersions were diluted to 10 $\mu gml^{-1}$ with deionised water, heated in a sealed tube to 95°C for 10 min., cooled to room temperature, and a 2 $\mu$l aliquot dropped onto a freshly cleaved mica surface. These samples were air-dried for 10 min. and then imaged by AFM. The supernatant samples were imaged under butanol and the insoluble deposit samples were imaged in air. The major obstacle to the reproducible imaging of polysaccharides and polysaccharide networks by AFM is the presence of strong adhesive forces between the tip and the substrate,

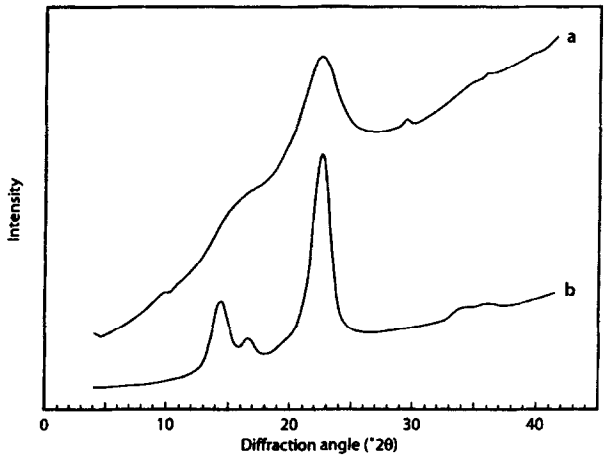


Fig. 2. X-ray powder diffraction patterns for: (a) insoluble deposit from PNG carrageenan (S-100) sample; (b) *Acetobacter xylinum* bacterial cellulose sample. Wavelength 0.154 nm.

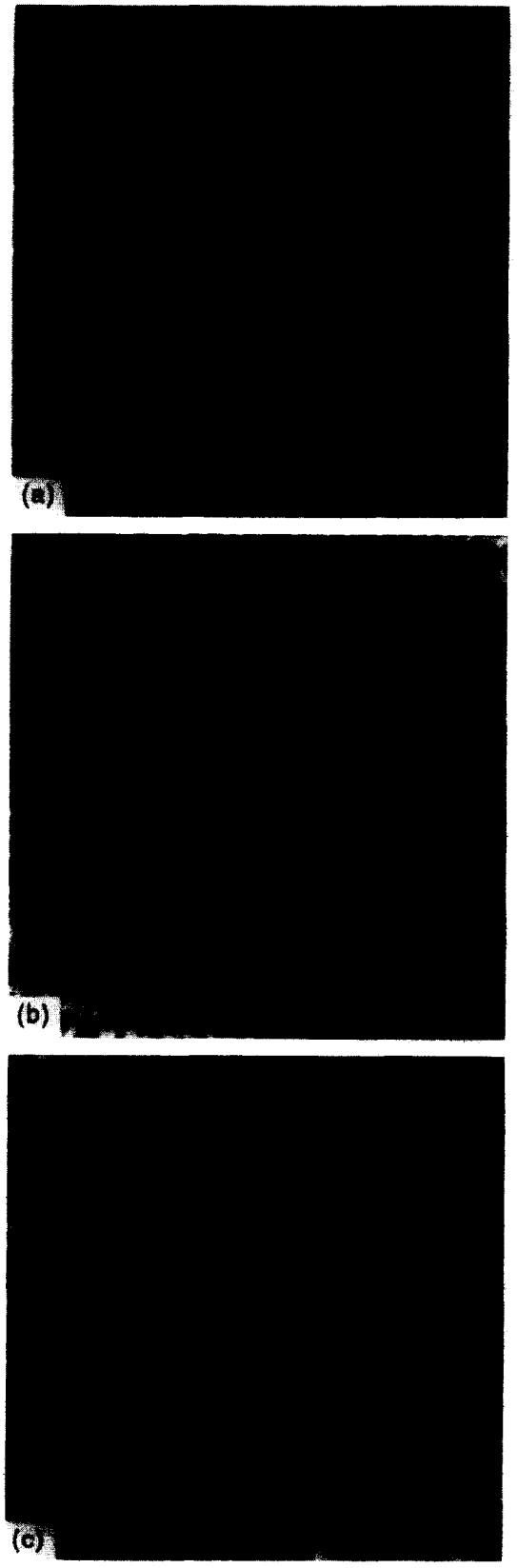


Fig. 3. AFM images of *iota* carrageenan samples: (a) refined sample, image size 900 × 900 nm; (b) supernatant from semi-refined (S-100) sample showing the predominant type of network, image size 1 × 1 $\mu$m; (c) supernatant from semi-refined (S-100) sample showing mixed networks, image size 700 × 700 nm.

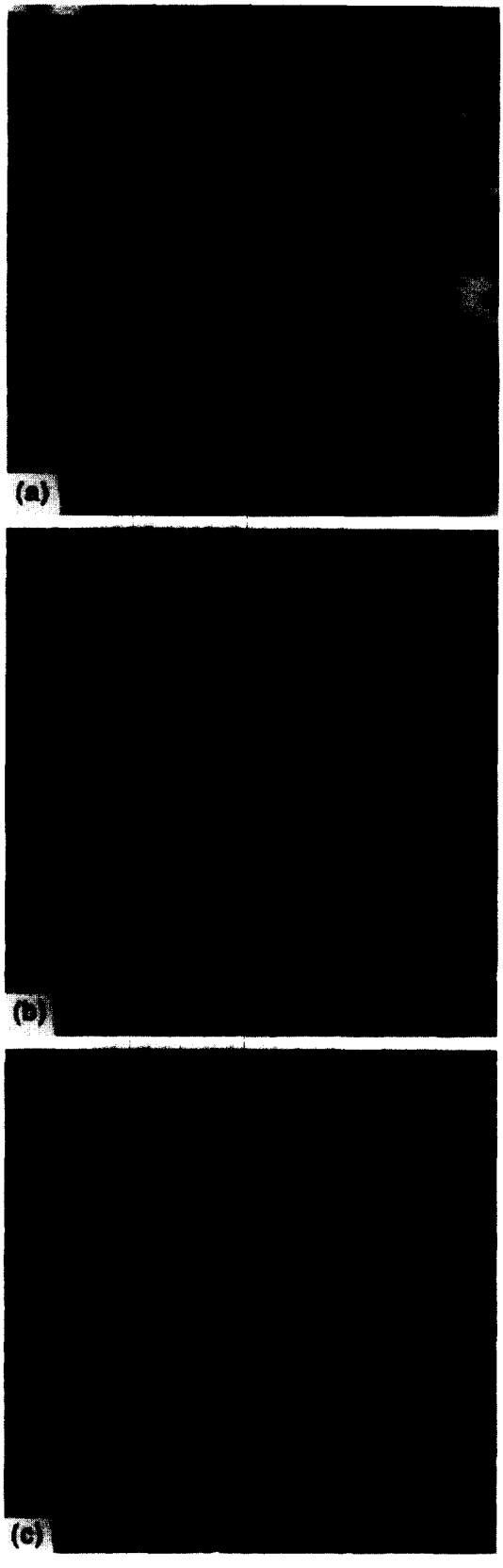


Fig. 4. AFM images of the same region of the insoluble deposit from semi-refined (S-100) *iota* carrageenan samples: (a) topographical image; (b) error signal mode image; (c) topographical image processed (smoothed over 10 pixels) as described in the text. Scan size 1.5 × 1.5 μm.

which can lead to sample damage or displacement upon scanning (Hansma & Hoh, 1994). Imaging individual polysaccharide molecules or weak networks in air is particularly difficult under normal humidity conditions; because adhesion arises due to coalescence of water layers on the tip and substrate. Such effects can be eliminated in a number of ways: reduced relative humidity, tapping (Zhjong et al., 1993; Dammer et al., 1995; Martin et al., 1995; Gunning et al., 1996) or constant force imaging under liquids (Hansma & Hoh, 1994; Kirby et al., 1996a). Imaging under butanol yields reproducible images for polysaccharides (Kirby et al., 1996a) and has been employed in the present studies. Tougher, more resilient networks, resist damage and can be imaged in air (Kirby et al., 1996b).

Refined *iota* carrageenan samples were purchased from Sigma Chemicals. The sample was ion exchanged into the sodium salt form as described by Belton et al. (1984). This sample was dispersed in water at a concentration of 1 $mgml^{-1}$ as described above. The resulting clear solution was diluted to 10 $\mu gml^{-1}$ and deposited onto freshly cleaved mica, using the procedure described for the PNG carrageenan samples. The air-dried deposits were imaged by AFM under butanol.

Fragments of cell walls from both potato and Chinese water chestnut plant tissue were extracted and purified by Drs K.W. Waldron and A. Ng using methods described in detail elsewhere (Coimbra et al., 1994; Kirby et al., 1996b). The fragments of cell walls were deposited onto freshly cleaved mica and imaged whilst still moist in air by AFM.

Bacterial cellulose samples were isolated from *A. xylinum* NRRL B42 (NCIB 40123) using methods described elsewhere (MacCormick et al., 1993). The gelatinous samples were dried in air, deposited onto freshly cleaved mica and imaged in air by AFM.

AFM images were obtained using an ECS (East Coast Scientific, Cambridge, UK) atomic force microscope operated in either the dc constant force or error signal modes. The apparatus and its operation are discussed in the PhD thesis of T.M.H. Wong (1991). Standard Nanoprobe (Digital Instrument, Santa Barbara, USA) cantilevers were used with a quoted force constant of 0.38 $Nm^{-1}$. Based on this quoted force constant the estimated imaging forces under butanol were between 3–8 nN.

X-ray diffraction studies were made using a Phillips Scientific PW 1820 vertical goniometer with an Anton Paar TTK camera, at the $CuK_\alpha$ wavelength of 0.154nm. Samples were scanned over the range 4.0–42.0°2$\theta$, at a speed of 0.005°2$\theta s^{-1}$, with a step size of 0.15°2$\theta$. Data was collected for the two fractions of S-100 (supernatant and deposit) and for dried *A.xylinum* bacterial cellulose samples.

## 3. Results and discussion

Aqueous dispersions of S-100 at 1 $mgml^{-1}$ were turbid and sedimented with time into a clearer supernatant and a

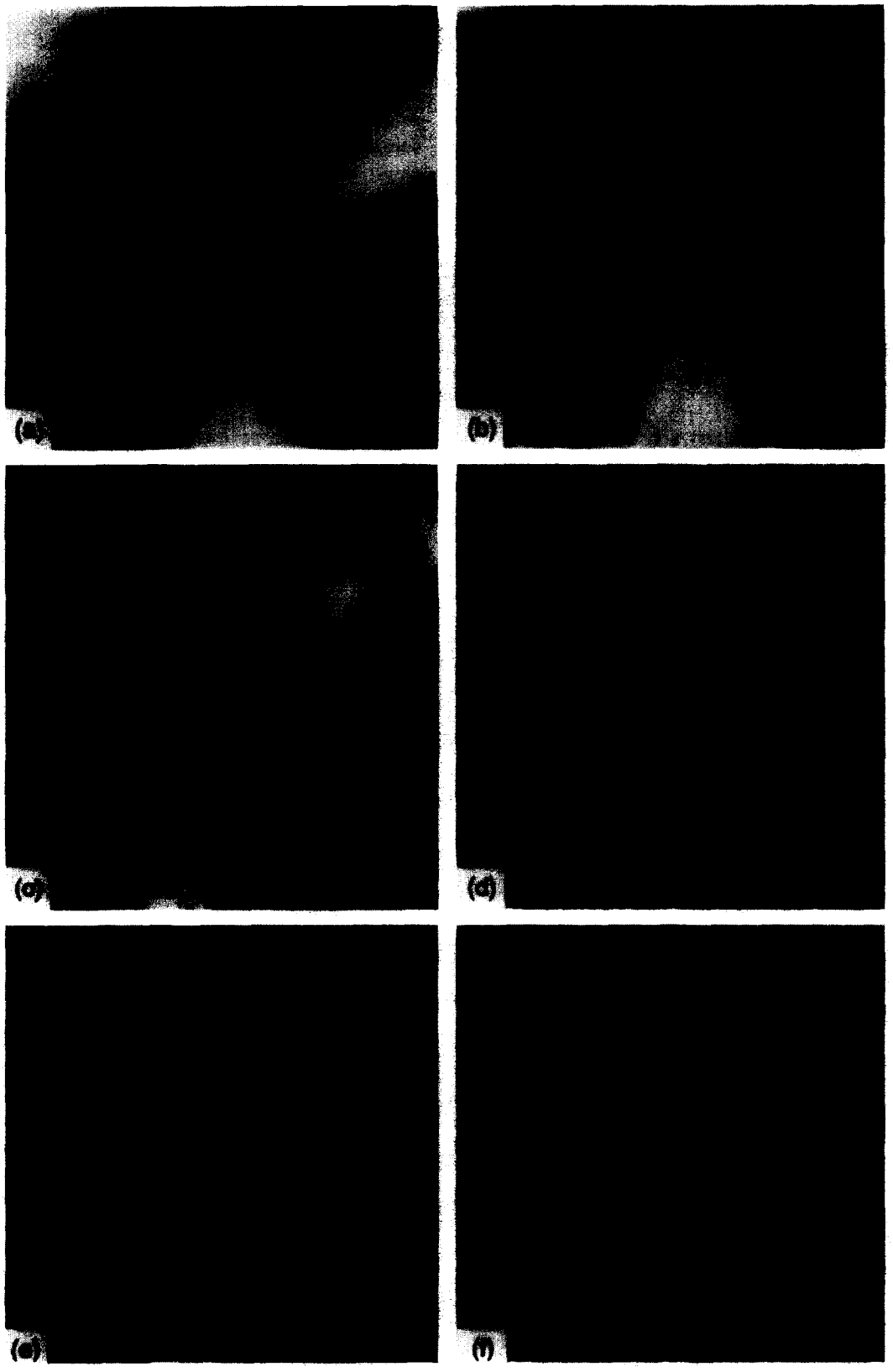

Fig. 5. AFM images of hydrated plant cell walls: (a) topographical image, potato; (b) topographical image, Chinese water chestnut; (c) error signal mode image, potato; (d) error signal mode image, Chinese water chestnut; (e) processed topographical image, potato; (f) processed (smoothed over 10 pixels) topographical image, Chinese water chestnut. Scan sizes 1 × 1 μm.

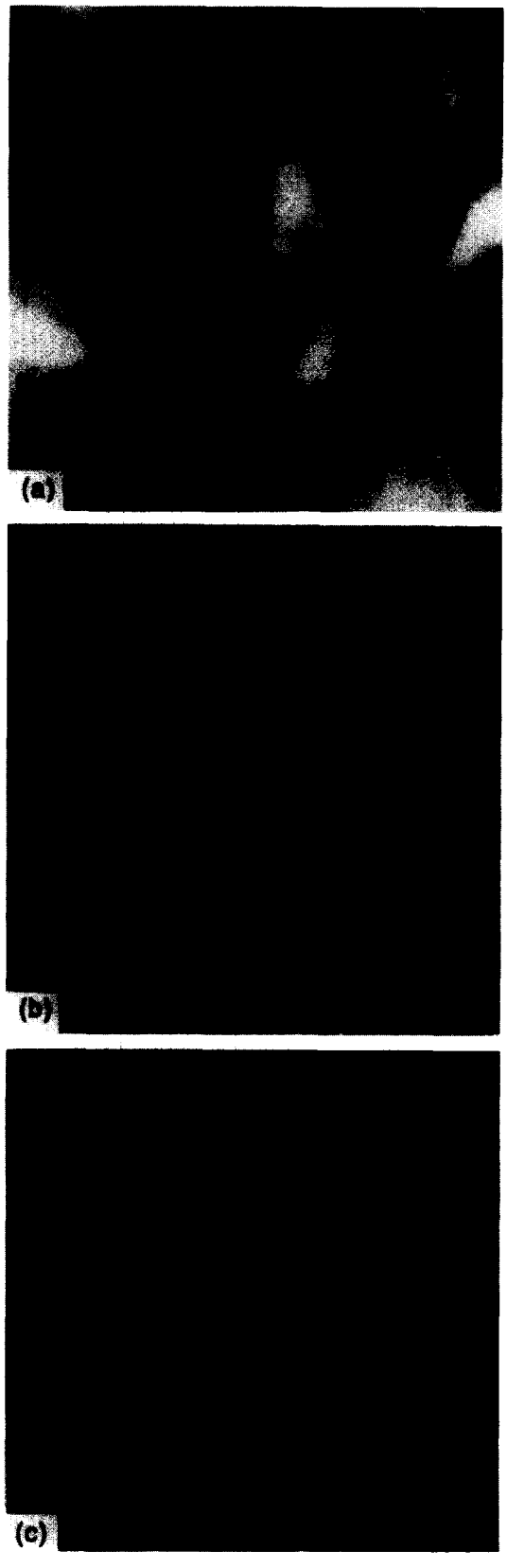


Fig. 6. AFM images of *A. xylinum* bacterial cellulose: (a) topographical image; (b) error signal mode image; (c) processed (smoothed over 10 pixels) topographical image. Scan size 8 × 8 μm.

more turbid insoluble deposit. The refined carrageenan prepared at the same concentration formed a clear aqueous sample. It is reasonable to assume that the insoluble deposit from the PNG carrageenan should be enriched in the cellulosic cell wall material. Fig. 2(a) shows an X-ray powder pattern obtained for the insoluble extract from the PNG carrageenan (S-100). The pattern shown is similar to that reported by Hoffman et al. (1995) for the insoluble extract from *E. cottoni* isolated using conditions similar to that used in the preparation of PNG carrageenans. They attribute this to a broadened cellulose I pattern characteristic of that found for most plant cell wall celluloses (Franz & Blaschek, 1993). Fig. 2(b) shows an X-ray powder diffraction pattern for *A. xylinum* bacterial cellulose. This shows a clearer, less broadened cellulose I pattern. Thus the insoluble residue does contain partially crystalline cellulose.

Fig. 3(a) shows an AFM image of refined *iota* carrageenan. The sample is deposited at a starting concentration of 10 $\mu g ml^{-1}$ and will become more concentrated when dried in air. Fig. 3(a) shows that such concentration has led to the formation of a polysaccharide network. The AFM image of the PNG *iota* carrageenan supernatant sample is similar in appearance (Fig. 3(b)) consistent with the formation of an *iota* carrageenan network. The network structure of Fig. 3(a) is homogeneous and composed of a continuous branched polymer network. The PNG network is similar in nature but does contain isolated regions (Fig. 3(c)) showing evidence for a different type of network. This second type of network contains fibres which are thicker and more rigid and it is possible that this additional network corresponds to the presence of small amounts of algal cell wall cellulose entrapped in the carrageenan network. This explanation is supported by images obtained from the largely cellulosic insoluble deposit from the PNG sample (Fig. 4). Fig. 4(a) shows a topographic AFM image of the network structure in the insoluble deposit preparation. The image shows bright and dark regions corresponding to peaks and troughs of the curved sample surface. The fibrous molecular structure is only just visible in the brighter regions of the image. The eye can not accommodate the large number of grey levels required to specify the rough sample surface and hence only perceives molecular structure in part of the image (Round et al., 1996). Similar effects have been observed in AFM studies of hydrated plant cell walls (Kirby et al., 1996b; Round et al., 1996). Error signal mode imaging (Putman et al., 1992) can be used to reveal the molecular structure in all of the image. The error signal mode image corresponding to Fig. 4(a) is shown in Fig. 4(b). A fibrous structure is revealed in which the fibres are stiff and rigid. Although error signal mode images reveal molecular structure they display changes in force gradient during scanning and are not true topographic images. However they justify further processing of topographic images. An improved image of the surface can be generated by the following procedure (Round et al., 1996): locally point smoothing the topographic image (Fig. 4(a)) over 10 pixels, thus averaging

out the high frequency molecular information to reveal the low frequency curvature of the surface, subtracting this smoothed image from Fig. 4(a) in order to produce a projection of the molecular structure onto a flat plane (Fig. 4(c)). This processed image reveals a layered fibrous structure similar to that observed for plant cell walls (Fig. 5) and bacterial cellulose (Fig. 6). Fig. 5 shows images of hydrated cell wall preparations from potato (Fig. 5(a,c,e)) and Chinese water chestnut (Fig. 5(b,d,f)) plant tissue. The cellulose microfibril structure, which is barely visible in the topographical images (Fig. 5(a,b)), is clearly evident in the error signal mode (Fig. 5(c,d)) and processed images (Fig. 5(e,f)). These images cover the spectrum of structures observed with plant tissue ranging from highly ordered and aligned cellulose microfibrils in water chestnut cell walls (Fig. 5(f)) to a more random structure seen in potato cell walls (Fig. 5(e)). Fig. 6 shows topographical (Fig. 6(a)), error signal mode (Fig. 6(b)) and processed topographical (Fig. 6(c)) images of extracellular *A. xylinum* bacterial cellulose. The PNG carrageenan insoluble residue samples (Fig. 4(a–c)) are similar to the random layered structures seen in potato cell walls (Fig. 5(e)). This may be characteristic of the algal cell wall, or possibly the alkali extraction procedure breaks down the side-by-side packing and alignment in the PNG samples, whilst leaving the microcrystalline fibres intact. The size and shape of the cellulose microfibrils is similar to that observed for higher plant cell wall preparations but quite different to the bacterial cellulose shown in Fig. 6. The present studies therefore suggest that the insoluble component in PNG carrageenan contains microcrystalline fibrous fragments of the seaweed cell wall. This insoluble fraction probably also contains some *iota* carrageenan. Imaging in air would disrupt weaker networks such as that expected to be formed by the *iota* carrageenan.

For *kappa* carrageenan, extracted using methods similar to those used in the preparation of PNG *kappa* carrageenan, the cellulosic component was found to increase the viscosity of hot 1% sols but not to significantly enhance the shear modulus of the gels formed on cooling to room temperature. Thus it would seem from the above AFM studies, and the work of Hoffman et al. (1995), that the cellulose component in PNG *iota* carrageenan will exist as swollen microgel-like particles interpenetrated by *iota* carrageenan networks.

## 4. Conclusions

The present studies confirm the presence of cellulose in PNG *iota* carrageenan. The cellulose is partially crystalline cellulose I. It is present as fibrous microcrystalline fragments of the seaweed cell wall. Preparative methods probably lead to partial disruption of the cell wall leading to loss of lateral alignment and ordering of the cellulosic fibrils. The swollen cell wall fragments would be expected to enhance the viscosity of hot sols. Such swollen particles should cause turbidity in the sols and gels. If the *iota* carrageenan networks can freely interpenetrate the cell wall fragments then the cellulosic components may not significantly enhance the shear modulus of the PNG carrageenan gels.

## Acknowledgements

All authors wish to thank Prof G.O. Phillips for advice and encouragement. Drs K.W. Waldron and A. Ng are thanked for preparing plant cell wall samples and Dr. M.L. Parker for providing the bacterial cellulose sample. The present studies were supported by the BBSRC through the CSG core grant to the Institute.

## References

Belton P.S., Chilvers G.R., Morris V.J., & Tanner S.F.(1984). *Int. J. Biol. Macromolecules, 6*, 303.

Coimbra M.A., Waldron K.W., & Selvendran R.R.(1994). *Carbohydr. Res., 252*, 245.

Dammer U., Popescu O., Wagner P., Anselmetti D., Guntherodt H.-J., & Misevic G.N.(1995). *Science, 267*, 1173.

Franz, G. & Blaschek, W. (1993) In *Methods in Plant Biochemistry, Carbohydrates*, Vol. 2, pp. 291. Academic Press, London.

Gunning A.P., Kirby A.R., & Morris V.J.(1996). *Ultramicroscopy, 63*, 1.

Hansma H.G., & Hoh J.H.(1994). *Ann. Rev. Biophys. Biomol. Structure, 23*, 115.

Hoffman R.A., Gidley M.J., Cooke D., & Frith W.J.(1995). *Food Hydrocolloids, 9*, 281.

Kirby A.R., Gunning A.P., & Morris V.J.(1996). *Bioploymers, 38*, 355.

Kirby A.R., Gunning A.P., Waldron K.W., Morris V.J., & Ng A.(1996). *Biophys. J., 70*, 1138.

Martin L.D., Vesenka J.P., Henderson E., & Dobbs D.L.(1995). *Biochemistry, 34*, 4610.

MacCormick C.A., Harris J.E., Gunning A.P., & Morris V.J.(1993). *J. Appl. Bacteriol., 74*, 196.

Percival, E. & McDowell, R.H. (1967) *Chemistry and Enzymology of Marine Algal Polysaccharides*, London, Academic Press.

Phillips, G. O. (1996) In *Gums and Stabilisers for the Food Industry*, Vol. 8, pp. 403. IRL Press, Oxford.

Putman C.A.J., van der Werf K.O., deGrooth B.G., van Hulst N.F., Greve J., & Hansma P.K.(1992). *SPIE Scanning Probe Microscopy, 1693*, 198.

Rees D.A.(1969). Advances Carbohydr. Chem. Biochem., *24*, 267.

Round A.N., Kirby A.R., & Morris V.J.(1996). *Microscopy and Analysis, 55*, 33.

Tye, R.J. (1994) In *Gums and Stabilisers for the Food Industry*, Vol. 7, pp. 125. IRL Press, Oxford.

Wong, T.M.H. (1991) Ph.D. Thesis, University of Cambridge, UK.

Zhjong Q., Inniss D., Kjoller K., & Elings V.B.(1993). *Surface Sci., 290*, L688.